A Parametric Study of Planar Cam-Roller Speed Reducers

Weimin Zhang* and **Jorge Angeles**
Department of Mechanical Engineering & Centre for Intelligent Machines
McGill University
817 Sherbrooke st. Montreal, QC, H3A 2K6 Canada
zweimin@cim.mcgill.ca angeles@cim.mcgill.ca

1 ABSTRACT

Speed-o-Cam, a family of speed-reduction mechanisms based on cams and pure-rolling contact, is currently under development at McGill University's Centre for Intelligent Machines. It is intended to replace gears and harmonic drives in applications where backlash, friction, and flexibility cannot be tolerated.
We focus on the pressure angle and the machinability of internal and external planar Speed-o-Cam layouts. In particular, this paper regards the pressure angle and the machinability as design constraints, while focusing on the Speed-o-Cam parameter optimization. A total of three design parameters, is investigated, so as to find the relationships between these parameters and the pressure angle, and the machinability of the cam plate. Optimum parameter values are thus obtained.

Une étude paramétrique de réducteurs de vitesse à cames et roulements

Une famille de réducteurs de vitesse à cames, nommée Speed-o-Cam, se trouve à l'heure actuelle sous développement au Centre McGill de recherches sur les machines intelligentes. Le but de ces travaux est de remplacer les réducteurs à engrenages et du type *harmonic drive* dans les applications où le jeu, le frottement et la flexibilité structurelle ne sont pas tolérés.
Nous nous concentrons sur l'étude de l'angle de pression et la fabricabilité des réducteurs planaires soit externes soit internes. Plus précisément, nous traitous l'angle de pression et conception, tout en visant l'optimisation des paramètres des mécanismes en question. Au total, nous recherchous trois paramètres de conception tout en établissant leur rapports géométriques avec l'angle de pression et la fabricabilité. Enfin nous obtenons des valeurs optimales desdits paramètres.

*Address all correspondence to this author.

2 Introduction

Speed-o-Cam, a cam-follower speed reducer, is an innovative design concept. As a new generation of mechanical transmissions, Speed-o-Cam offers advantages such as low friction, low backlash, high stiffness and high machinability with general-purpose CNC machine tools. All this means that Speed-o-Cam can compete with traditional speed reducers. It is expected that Speed-o-Cam will replace spur and helicoidal gears, bevel gears and rack-and-pinions in robotic mechanical systems and other precision-demanding mechanical systems.

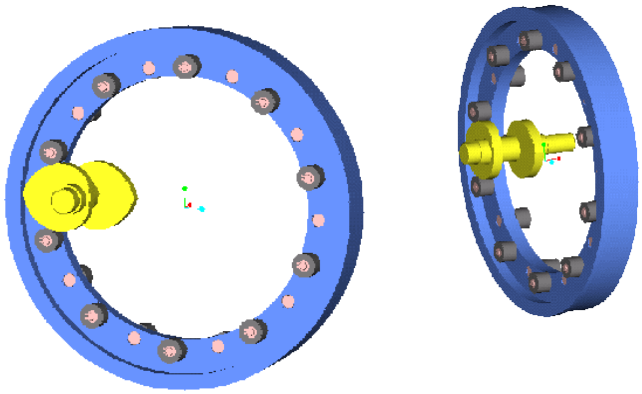

Figure 1: Two distinct views of internal Speed-o-Cam

Figures 1 and 2 show typical planar internal and external Speed-o-Cam embodiments. The theory behind these layouts is available in (González-Palacios and Angeles, 1993). The design method can be found in (Lee, 2001).The underlying research has reached a mature stage. Figure 3 is a prototype of spherical Speed-o-Cam, Fig. 4 showing two prototypes of planar Speed-o-Cam.

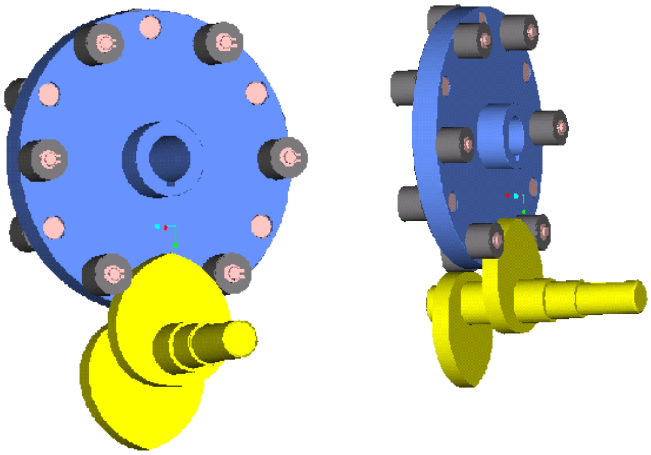

Figure 2: Two distinct views of external Speed-o-Cam

In this paper, the maximum pressure angle and the machinability of planar Speed-o-Cam are regarded as design specifications. Unlike gear transmissions, in which the pressure angle is constant, the pressure angle of Speed-o-Cam varies within a broad range. The paper thus focuses on the factors that affect the pressure angle and ease

Figure 3: A prototype of spherical Speed-o-Cam

the machinability of the cam plate with evenly distributed machining errors. It is noteworthy that the pressure angle of planar oscillating-follower cam mechanisms attains the same value when measured either at the cam profile or at the pitch curve (Angeles and López-Cajún, 1991). This means that the radius of the roller does not affect the presure-angle variation.

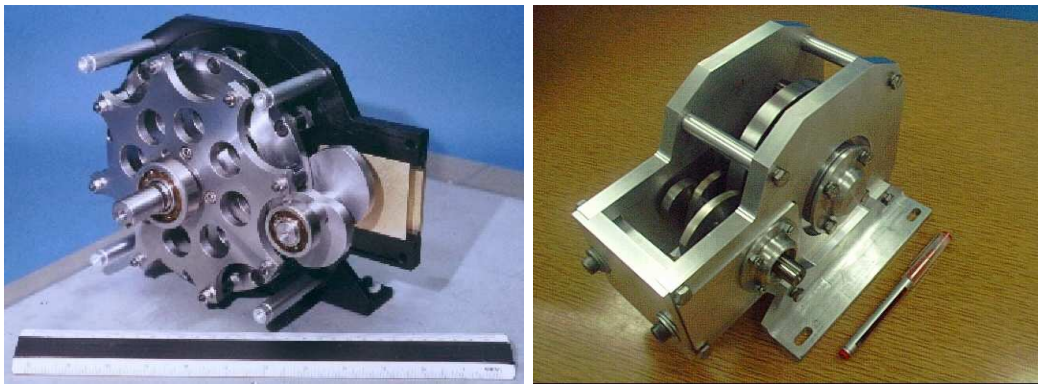

(a) The concave planar Speed-o-Cam (b) The convex planar Speed-o-Cam

Figure 4: Prototypes of planar Speed-o-Cam

3 The Determination of The Cam Profile

As shown in Fig. 5, the Cartesian coordinates of the cam profile for planar Speed-o-Cam in the u-v plane can be readily obtained as (González-Palacios and Angeles,

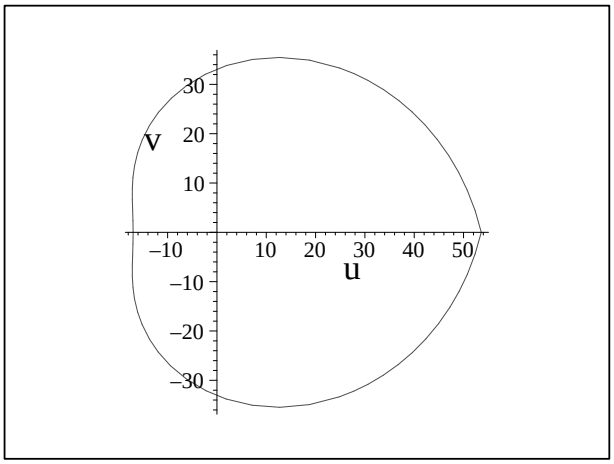

Figure 5: Cam profile

1993)

$$u(\psi) = b_2 \cos\psi + (b_3 - a_4)\cos(\psi - \delta) \tag{1a}$$

$$v(\psi) = -b_2 \sin\psi - (b_3 - a_4)\sin(\psi - \delta) \tag{1b}$$

where

$$b_2 = \frac{\tilde{\phi}'}{\tilde{\phi}' - 1} a_1 \tag{2a}$$

$$b_3 = \sqrt{(a_3 \cos\tilde{\phi} + a_1 - b_2)^2 + (a_3 \sin\tilde{\phi})^2} \tag{2b}$$

$$\delta = \arctan\left(\frac{a_3 \sin\tilde{\phi}}{a_3 \cos\tilde{\phi} + a_1 - b_2}\right) \tag{2c}$$

For the internal planar Speed-o-Cam, the input-output relationship takes the form

$$\tilde{\phi} = \pi\left(1 - \frac{1}{N}\right) + \frac{\psi}{N} \tag{3a}$$

while the external planar Speed-o-Cam entails an input-output relationship of the form

$$\tilde{\phi} = -\left[\pi\left(1 - \frac{1}{N}\right) + \frac{\psi}{N}\right] \tag{3b}$$

with the notation described below:
a_1 : distance between the input and output axes;
a_3 : distance between the output and roller axes;
a_4 : radius of the roller;
N : number of indexing steps, its reciprocal being the speed-reduction ratio;
ψ : angle of rotation of the cam;
$\tilde{\phi}$: angular displacement of the follower;
$\tilde{\phi}'$: derivative of the angular displacement of the follower with respect to ψ.

Figure 6 shows the profile of the cam with $0 \leq \psi \leq 2\pi$, in which the profile does not close. An extended angle Δ is introduced so that the cam profile closes, as shown in Fig. 5, with $-\Delta \leq \psi \leq 2\pi + \Delta$. Angle Δ is obtained as a root of the equation

$$v(-\Delta) = 0 \qquad (4)$$

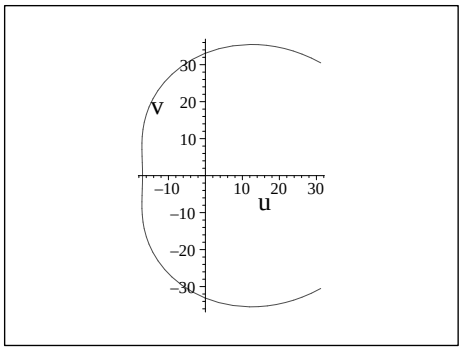

Figure 6: Cam profile in $0 \leq \psi \leq 2\pi$

4 The Computation of the Pressure Angle

The pressure angle μ is that between the line of motion of the follower contact point and the normal to the cam surface at the same point. The pressure angle has two major effects on the mechanical transmission. First, the higher the pressure angle, the smaller the component of the force transmitted to and used to drive the follower. Another aspect is the radial load on the bearings. A high pressure angle means a heavy load transmitted to the bearings and a short life of the bearings.

The pressure angle is computed from (González-Palacios and Angeles, 1993)

$$\mu = \arctan\left(\frac{a_3(\phi' - 1) - a_1 \cos\phi}{a_1 \sin\phi}\right) \qquad (5)$$

Figure 7 is a typical plot of the pressure angle of internal Speed-o-Cam with $a_1 = 100$mm, $a_3 = 128$mm, $a_4 = 8$mm, and $N = 10$. It is apparent from the figure that the pressure angle varies over a wide range of values.

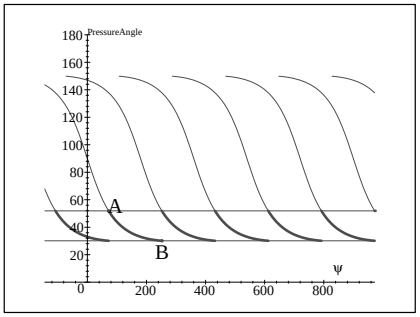

Figure 7: The pressure angle distribution for internal Speed-o-Cam with $a_1 = 100$mm, $a_2 = 128$mm, $a_4 = 8$mm, and $N = 10$

When $0° \leq \mu < 90°$, the power transmission is from the cam to the follower, Speed-o-Cam being said to operate under positive action, or PA (Gonzalez-Palacios and Angeles, 1993). On the contrary, when $90° \leq \mu < 180°$, the power transmission is from the follower to the cam, Speed-o-Cam operating under negative action, or NA.

In order to ensure that there is at least one positive action or PA any time, two conjugate cam-follower pairs are used in Speed-o-Cam, as shown in Figs. 1 and 2.

In Figure 7, the one pair offers PA from A to B. Before point A, the other pair is engaged under a lower pressure angle and, therefore, can take the load. Alternatively, the two pairs offer PA and drive the follower all the time. As shown in Fig. 7, the highlighted lines indicate the PA delivered alternatively by the two pairs. Below we define and determine three figures of merit between A and B: the maximum pressure angle, the minimum pressure angle, and the root-mean-square (rms) of the pressure angle distribution. Henceforth, we will denote by ψ_A and ψ_B the values attained by ψ at points A and B, respectively. Pressure angle values at A and B will be indicated likewise.

4.1 The Maximum Pressure Angle

The maximum pressure angle μ_{max} corresponds to the maximum contact compressive stress; it thus has a great effect on the mechanism performance under three primary modes of failure, which are breakage, pitting, and scoring. Usually, the curve from

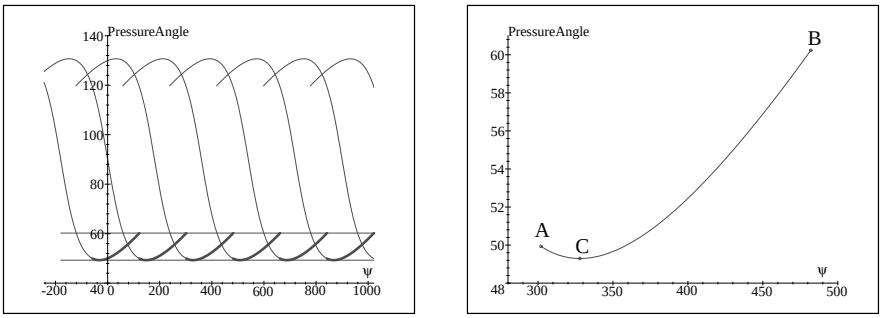

(a) (b)

Figure 8: The pressure angle for external Speed-o-Cam with $a_1 = 100$mm, $a_3 = 230$mm, $a_4 = 8$mm, and $N = 3$, (a) a whole cycle; (b) details on $\psi_A \leq \psi \leq \psi_B$

ψ_A to ψ_B, where PA takes place, is monotonically decreasing, as shown in Fig. 7, so that $\mu_{max} = \mu_A = \mu(\psi_A)$. However, sometimes the curve is not monotonic. Figure 8a shows the plot of the pressure angle distribution of external Speed-o-Cam with: $a_1 = 100$mm, $a_3 = 230$mm, $a_4 = 8$mm and $N = 3$, while Fig. 8b is obtained by zooming-in on Fig. 8a with $\psi_A \leq \psi \leq \psi_B$. The curve decreases from ψ_A and reaches its minimum at $\psi = \psi_C$; it then grows up to ψ_B. It is clear that in the case of Fig. 8, $\mu_{max} = \mu_B = \mu(\psi_B)$. Considering both Figs. 7 and 8, μ_{max} is defined as the largest between μ_A and μ_B, i.e.

$$\mu_{max} = \max\{\mu_A, \quad \mu_B\} \tag{6}$$

where

$$\psi_A = \pi + \Delta \tag{7a}$$
$$\psi_B = 2\pi + \Delta \tag{7b}$$

and Δ is obtained from eq.(4).

4.2 The Minimum Pressure Angle

In the case of Fig. 7, $\mu_{min} = \mu_B = \mu(\psi_B)$. In Fig. 8, however, $\mu_{min} = \mu_C = \mu(\psi_C)$. Therefore, μ_{min} is found as the solution to the optimization problem

$$\mu_{min} = \min_{\psi} \mu(\psi) \tag{8a}$$

where ψ is subject to

$$\psi_A \leq \psi \leq \psi_B \tag{8b}$$

If we let the minimum value of $\mu(\psi)$ occur at $\psi = \psi_C$, then ψ_C verifies

$$\mu'(\psi_C) = 0, \qquad \psi_C \in [\psi_A, \quad \psi_B] \tag{9}$$

4.3 The Root-Mean-Square Value of the Pressure Angle

The root-mean-square (rms) value of the pressure angle between ψ_A and ψ_B corresponds to the mean contact compressive stress; it has therefore a great effect on the mechanism pitting and scoring. The rms of $\mu(\psi)$ is given by

$$\mu_{rms} = \sqrt{\frac{1}{\pi} \int_{\pi+\Delta}^{2\pi+\Delta} \mu^2 \, \mathrm{d}\psi} \tag{10}$$

5 Cam Curvature and Cam Machinability

The curvature of a contour in terms of a parameter ψ is available in any calculus textbook – e.g. Bers, 1969 – as

$$\kappa = \frac{v'(\psi)u''(\psi) - u'(\psi)v''(\psi)}{((v'(\psi))^2 + (u'(\psi))^2)^{\frac{3}{2}}} \tag{11}$$

By substituting eq.(1) into eq.(11) and simplifying it, the curvature of the cam plate can be obtained as

$$\kappa = \frac{f_1}{a_1 f_2 - a_4 f_1} \tag{12}$$

where

$$f_1 = r^2(1-\tilde{\phi}')^3 + r[(1-\tilde{\phi}')(2-\tilde{\phi}')\cos\tilde{\phi} + \tilde{\phi}''\sin\tilde{\phi}] + 1 \tag{13a}$$

$$f_2 = [r^2(1-\tilde{\phi}')^2 + 2r(1-\tilde{\phi}')\cos\tilde{\phi} + 1]^{\frac{3}{2}} \tag{13b}$$

$$r = \frac{a_3}{a_1} \tag{13c}$$

In order to generate a fully-convex cam profile for an internal Speed-o-Cam, parameter r must satisfy (Lee, 2001)

$$r \geq \frac{1}{1-1/N} \tag{14a}$$

Likewise, for an external Speed-o-Cam, r must satisfy.

$$r \leq \frac{1}{1+1/N} \tag{14b}$$

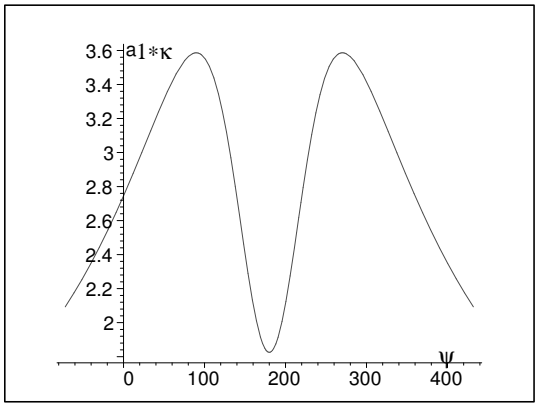

Figure 9: Dimensionless curvature for internal Speed-o-Cam with $r = 1.28$mm, $a_1 = 100$mm, $a_4 = 8$mm, and $N = 10$

It is convenient to use $a_1\kappa$, the dimensionless curvature, instead of κ itself. Figure 9 is the dimensionless curvature distribution of the internal Speed-o-Cam, with $a_1 = 100$mm, $a_3 = 128$mm, $a_4 = 8$mm, and $N = 10$.

From Fig. 9, it is apparent that the curvature attains one minimum and two maxima throughout the cam profile. The extent of curvature fluctuation determines the machinability of the cam plate. Undoubtedly, among all closed curves, the circle is the easiest to manufacture because its curvature is constant. In order to measure how *machinable* a cam profile is, machinability, denoted by m, was introduced by Lee, (2001). Machinability is defined as

$$m = e^{-L} \times 100\% \tag{15}$$

where L, the loss of circularity, is defined as the absolute value of the standard deviation σ of the curvature devided by the curvature mean value $\bar{\kappa}$, i.e.,

$$L = \left|\frac{\sigma}{\bar{\kappa}}\right| \tag{16}$$

where

$$\bar{\kappa} = \frac{1}{2\pi + 2\Delta}\int_{-\Delta}^{2\pi+\Delta} \kappa \, \mathrm{d}\psi \tag{17a}$$

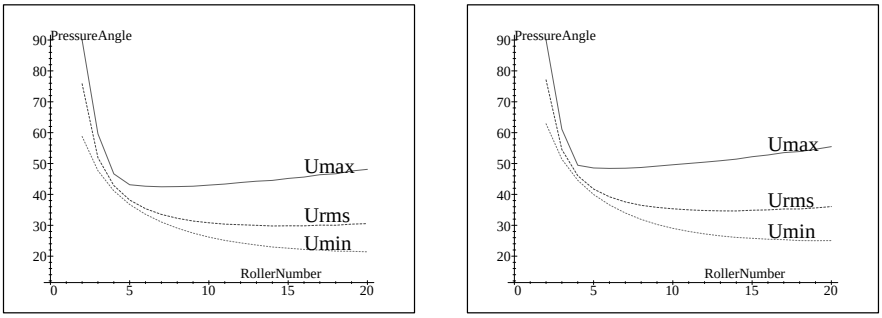

(a) (b)

Figure 10: Pressure-angle variations for internal Speed-o-Cam for: (a) $m = 70\%$; (b) $m = 80\%$

and σ is the standard deviation of the curvature from its mean value, i.e.,

$$\sigma = \sqrt{\frac{1}{2\pi + 2\Delta} \int_{-\delta}^{2\pi+\delta} (\kappa - \bar{\kappa})^2 \, \mathrm{d}\psi} \tag{17b}$$

From the above definition,

$$L \geq 0 \tag{18}$$

and hence,

$$0 < m \leq 100\% \tag{19}$$

From eq.(15), in the case of a circle, $L = 0$, and hence, $m = 100\%$. Apparently, the larger L, which means the more irregular the contour is, the smaller m. Therefore, m can properly represent the machinability of a cam plate.

6 The Relationship Between the Number of Follower Rollers and the Pressure Angle

Table 1, which corresponds to Fig. 10, shows the relationship between various values of N, μ_{max}, μ_{rms}, and μ_{min} for internal Speed-o-Cam. The parameter r, i.e. a_3/a_1, is chosen carefully so as to give $m \approx 70\%$, and 80%, respectively. From the table and the corresponding figure, it can be found that the pressure angle is very sensitive to the number of follower rollers. When N increases, μ_{max} declines sharply at first, reaching a minimum at value of N between 6 and 7, and then rises slowly. Similarly, μ_{rms} falls rapidly and goes up slightly, reaching a minimum when $N = 14$. However, μ_{min} decreases monotonically. Considering the behavior of the pressure-angle variation, it is recommended that N lies between 6 and14 for internal Speed-o-Cam.

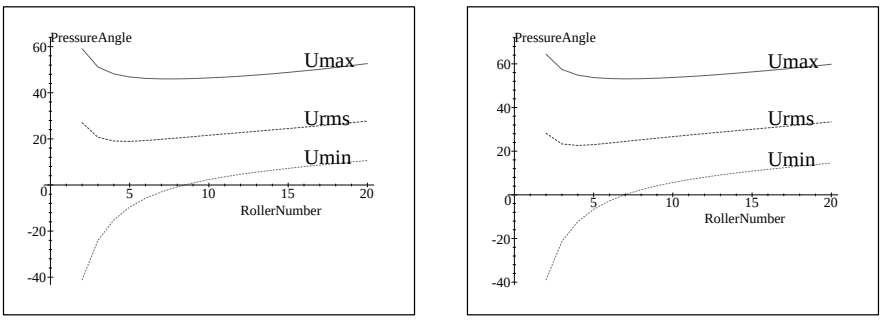

(a) (b)

Figure 11: Pressure-angle variations for external Speed-o-Cam for: (a) $m = 70\%$; (b) $m = 80\%$

Table 2, which corresponds to Fig. 11, illustrates the forgoing relationships for external Speed-o-Cam, when $m \approx 70\%$, and 80%, respectively. The tendencies of μ_{max}, μ_{rms}, and μ_{min} are simular to those of internal Speed-o-Cam. When N lies between 7 and 8, and between 4 and 5, μ_{max} and μ_{rms} attain their minima, respectively. Therefore, it is suggested that N be kept between 6 and 10 for external Speed-o-Cam.

7 The Relationship Among r, μ, and m

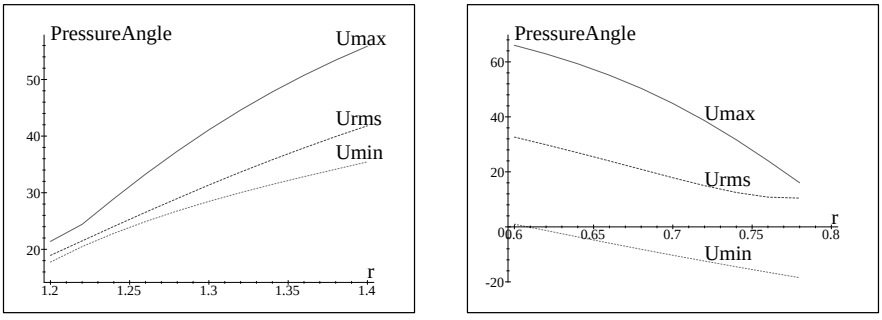

(a) (b)

Figure 12: r vs. μ plot for: (a) internal Speed-o-Cam; (b) external Speed-o-Cam

As for the pressure angle and machinability, r is the most important of all parameters. Figure 12a shows the relationships of interest between the pressure angle

and the parameter r for internal Speed-o-Cam when $a_1 = 100$mm, $a_4 = 8$mm, and $N = 8$. Figure 12b applies to external Speed-o-Cam when $a_1 = 100$mm, $a_4 = 8$mm, and $N = 5$. For internal Speed-o-Cam, μ_{max}, μ_{rms}, and μ_{min} grow with r almost linearly. Contrary to its internal counterpart, μ_{max}, μ_{rms}, and μ_{min} decrease as r grows for external Speed-o-Cam.

Figure 13 depicts the relationships between r and m. Figure. 13a illustrates that the

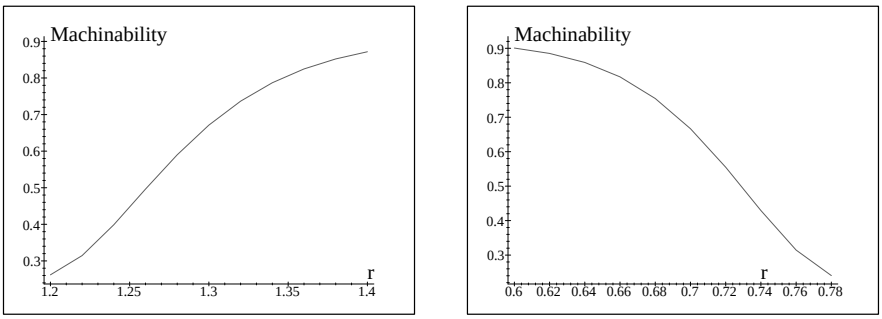

(a) (b)

Figure 13: r vs. m plot for: (a) internal Speed-o-Cam; (b) external Speed-o-Cam

machinability grows with r in internal Speed-o-Cam, while m follows the contrary pattern in the external Speed-o-Cam, as shown in Fig. 13b.

An interesting phenomenon is found in Figs. 12 and 13. It is apparent here that in

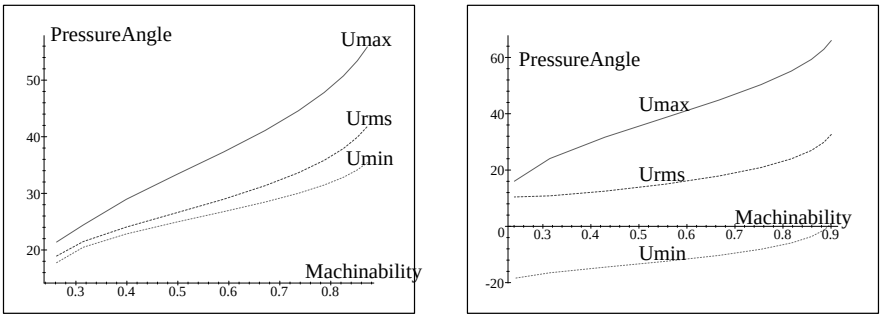

(a) (b)

Figure 14: m vs. μ plot for: (a) internal Speed-o-Cam; (b) external Speed-o-Cam

internal and external Speed-o-Cam, the pressure angle and the machinability observe similar trends, as shown in Fig. 14. This is bad news because it is expected that Speed-o-Cam has the characteristics of both low pressure angle and high machinabil-

ity. Now, designers have to be careful to keep a balance between pressure angle and machinability.

8 The Relationship Between Machinability and a_4

Let the pitch curve have a curvature $\kappa_p(\psi)$. The relationship with κ is given by (Angeles and López-Cajún, 1991)

$$\kappa = \frac{\kappa_p}{1 - a_4\kappa_p} \tag{20a}$$

whence

$$\kappa_p = \frac{\kappa}{1 + a_4\kappa} \tag{20b}$$

If we rewrite eq.(20b) in terms of the corresponding radii of curvature, ρ_p and ρ, respectively, then a simpler relation is obtained, namely,

$$\rho_p = a_4 + \rho \tag{21}$$

which means that the two radii of curvature differ by one constant. As a result, both $\rho_p(\psi)$ and $\rho(\psi)$ have the same standard deviation, but their mean values differ by one constant a_4, i.e.

$$\bar{\rho_p} = a_4 + \bar{\rho} \tag{22}$$

Therefore, from eq.(15) and eq.(16), a_4 affect the cam-plate machinability. However, considering that a_4 varies within a narrow range because of space availability and stiffness, the effect of a_4 is so small that it can be ignored.

Table 1: The relationship of N with key pressure-angle values for internal Speed-o-Cam

$m = 70\%$					$m = 80\%$				
N	r	$\mu_{\mathbf{max}}(^\circ)$	$\mu_{\mathbf{rms}}(^\circ)$	$\mu_{\mathbf{min}}(^\circ)$	N	r	$\mu_{\mathbf{max}}(^\circ)$	$\mu_{\mathbf{rms}}(^\circ)$	$\mu_{\mathbf{min}}(^\circ)$
2	3.859	90.00	75.84	58.78	2	4.388	90.00	77.10	62.88
3	2.228	59.62	51.89	47.68	3	2.404	61.09	54.51	51.39
4	1.771	46.65	42.88	41.16	4	1.872	49.44	46.06	44.58
5	1.560	43.13	38.18	36.75	5	1.631	48.56	41.74	39.97
6	1.440	42.66	35.39	33.56	6	1.495	48.42	39.22	36.61
7	1.362	42.47	33.53	31.06	7	1.407	48.49	37.57	33.98
8	1.308	42.54	32.28	29.10	8	1.346	48.72	36.47	31.89
9	1.268	42.66	31.37	27.47	9	1.302	49.16	35.81	30.28
10	1.238	43.02	30.81	26.17	10	1.268	49.60	35.34	29.02
11	1.214	43.35	30.38	25.10	11	1.241	50.03	35.01	28.02
12	1.195	43.85	30.17	24.30	12	1.219	50.44	34.78	27.21
13	1.179	44.28	30.00	23.61	13	1.201	50.91	34.67	26.57
14	1.165	44.54	29.77	22.97	14	1.186	51.43	34.65	26.07
15	1.154	45.17	29.84	22.58	15	1.174	52.20	34.88	25.79
16	1.144	45.61	29.82	22.18	16	1.163	52.76	34.94	25.48
17	1.136	46.37	30.06	21.98	17	1.154	53.52	35.28	25.35
18	1.128	46.67	30.01	21.64	18	1.145	53.88	35.29	25.05
19	1.122	47.57	30.38	21.58	19	1.138	54.62	35.63	25.00
20	1.116	48.12	30.53	21.41	20	1.132	55.47	36.07	25.04

Table 2: The relationship of N with key pressure-angle value for external Speed-o-Cam

$m = 70\%$					$m = 80\%$				
N	r	$\mu_{\mathbf{max}}(^\circ)$	$\mu_{\mathbf{rms}}(^\circ)$	$\mu_{\mathbf{min}}(^\circ)$	N	r	$\mu_{\mathbf{max}}(^\circ)$	$\mu_{\mathbf{rms}}(^\circ)$	$\mu_{\mathbf{min}}(^\circ)$
2	0.4474	59.10	27.04	-41.11	2	0.4129	64.39	28.22	-38.90
3	0.5632	51.15	20.71	-24.04	3	0.5311	57.45	23.32	-21.40
4	0.6395	48.17	19.06	-15.12	4	0.6101	54.85	22.60	-12.28
5	0.6931	46.84	18.91	-9.58	5	0.6663	53.71	23.00	-6.63
6	0.7327	46.23	19.27	-5.78	6	0.7080	53.25	23.71	-2.73
7	0.7630	46.02	19.81	-2.98	7	0.7402	53.12	24.47	0.14
8	0.7870	46.01	20.38	-0.83	8	0.7657	53.21	25.23	2.37
9	0.8064	46.15	20.97	0.90	9	0.7865	53.43	25.97	4.17
10	0.8223	46.44	21.57	2.34	10	0.8035	53.76	26.67	5.68
11	0.8357	46.76	22.14	3.55	11	0.8178	54.17	27.37	6.97
12	0.8470	47.19	22.72	4.62	12	0.8300	54.62	28.04	8.09
13	0.8567	47.68	23.30	5.56	13	0.8404	55.16	28.72	9.12
14	0.8651	48.22	23.88	6.42	14	0.8495	55.71	29.37	10.03
15	0.8724	48.82	24.47	7.21	15	0.8574	56.32	30.03	10.89
16	0.8788	49.49	25.08	7.95	16	0.8644	56.94	30.68	11.67
17	0.8845	50.18	25.68	8.64	17	0.8706	57.59	31.34	12.42
18	0.8895	50.95	26.33	9.31	18	0.8760	58.34	32.05	13.17
19	0.8939	51.80	27.02	9.98	19	0.8809	59.07	32.74	13.88
20	0.8979	52.65	27.70	10.62	20	0.8853	59.83	33.44	14.56

Conclusions

The pressure angle and the machinability of Speed-o-Cam was the subject of this paper: the underlying principles were applied to the optimum design of the planar external and internal layouts of Speed-o-Cam. In fact, the pressure angle and the machinability are such important indices that, to some extent, they determine the quality of the design. In analyzing the pressure angle, we focus on three figures of merit: the maximum pressure angle; the minimum pressure angle; and the root-mean-square value of the pressure angle. The report also applies the concept of the *machinability*, introduced by Lee, 2001. By analyzing the pressure angle and the machinability, as well as all parameters that affect them, their sensitivities and tendencies to these parameters are illustrated.

- For internal Speed-o-Cam, the optimum number of rollers lies in the range of 6 to 14, while the number is 4 to 10 for external Speed-o-Cam.
- When the ratio a_3/a_1 rises, both the pressure angle and the machinability of internal Speed-o-Cam grow, while both decrease in external Speed-o-Cam.
- For both internal and external Speed-o-Cam, when the pressure angle grows, the machinability grows almost linearly.
- The radius of the roller, a_4, does not affect the machinability of either the internal or the external layouts of Speed-o-Cam.

The designer should first decide on the number of follower rollers N, a basic design parameter, which is primarily determined by the Speed-o-Cam ratio and should comply with the above constraints. Then, the designer should obtain the distance between the input and the output axes a_1, also a basic design parameter, which is dictated by the space availability and the transmitted load. The third step is the most important: this consists in choosing the distance a_3 between the output and the roller axes, equivalent to parameter r when the center-distance a_1 is given. The designer should be careful because both the pressure angle and the machinability are highly sensitive to this parameter. Since the pressure angle and the machinability exhibit opposite tendencies with respect to r, a balance should be reached. Finally, the radius of the roller a_4 is chosen. The stiffness and the space availability, instead of the pressure angle and machinability, are the main elements considered.

References

González-Palacios, M. A. and Angeles, J., 1993, *Cam Synthesis*, Kluwer Academic Publishers, Dordrecht, Boston.

Lee, M. K., 2001, *"Design for Manufacturability of Speed-Reduction Cam Mechanisms"*, Master's thesis, Dept. of Mechanical Engineering, McGill University.

Bers, L., 1969, *Calculus*, Holt, Rinehart and Winston, Inc.

González-Palacios, M. A. and Angeles, J., 1999, *The Design of a Novel Mechanical Transmission for Speed Reduction*, ASME J. of Mechanical Design, Vol.121, NO.4.

Angeles, J. and González - Palacios, M. A., 2002, *United States Patent*, Patent No.: US 6,382,038 B2.

Erik Oberg, Franklin D. Jones, and Holbrook L. Horton, 1988, *Machinery's Hand Book, 23 Revised Edition*, Industrial Press Inc., New York.

Teng, C., 1996, *Force-and-Motion Transmission Between Intersecting Axes with Speed Rectification and Reduction*, Master's Thesis, Dept. of Mechanical Engineering, McGill University.

Teng, C., Angeles, J., and Khader, K., 1996, *The Synthesis of a Transmission with Intersecting Axes for Rectifying and Reducing a Periodic Speed*, 1996 ASME Design Engineering Technical Conference and Computers in Engineering Conference.

Müller, H.W., 1982, *Epicyclic Drive Trains, Analysis, Synthesis, and Applications.* Wayne State University Press, Detroit.

Ullman, David G. 1997. *The Mechanical Design Process*, Second Edition, McGraw-Hill, Boston, Massachusetts.

Norton, R.L. 2002 *Cam Design and Manufacturing Handbook.* Industrial Press, New York.

Oberg, E., Jones, F. D. and Horton, H. L. 1988. *Machinery's Handbook*, 23rd Edition. Industrial Press Inc. New York.

Norton, R.L. 1999. *Design of Machinery*, Second Edition, WCB McGraw-Hill, New York.